JOURNAL OF SOLID STATE CHEMISTRY **125,** 13–18 (1996)
ARTICLE NO. 0258

Gibbs Energy of Formation of $Cu_2Yb_2O_5$ and Thermodynamic Stability of $Cu_2R_2O_5$ (R = Tb–Lu)

G. M. Kale

Department of Mining and Mineral Engineering, University of Leeds, Leeds LS2 9JT, United Kingdom

Received October 18, 1995; in revised form April 10, 1996; accepted April 15, 1996

The electromotive force (emf) of the solid oxide electrochemical cell,

$$(-)\mathrm{Pt/Cu_2O + Yb_2O_3 + Cu_2Yb_2O_5//(CaO)ZrO_2//O_2}\ (P = 0.0212\ \mathrm{MPa})/\mathrm{Pt}(+),$$

has been measured between 960 and 1320 K. Based on the measured emf of the above cell as a function of temperature, the Gibbs energy change for the reaction

$$2Cu_2O(s) + 2Yb_2O_3(s) + O_2(g) \rightarrow 2Cu_2Yb_2O_5(s)$$

is obtained as

$$\Delta G^\circ = -231{,}225 + 151.847T\ (\pm 200)\ \mathrm{J\ mol^{-1}}.$$

The Gibbs energy change for the above reaction when combined with that for Cu_2O + CuO equilibrium from the literature gives, for the reaction

$$2CuO(s) + Yb_2O_3(s) \rightarrow Cu_2Yb_2O_5(s),$$
$$\Delta G^\circ = 17{,}128 - 20.07T\ (\pm 100)\ \mathrm{J\ mol^{-1}}.$$

It can be seen that the formation of $Cu_2Yb_2O_5$ from the component oxides is endothermic. Since $Cu_2Yb_2O_5$ is an entropy stabilized compound and its formation is endothermic from component oxides, $Cu_2Yb_2O_5$ is thermodynamically unstable relative to its component oxides below 853 K. Earlier we reported the Gibbs energy of formation of $Cu_2Dy_2O_5$, $Cu_2Ho_2O_5$, and $Cu_2Er_2O_5$ from CuO and R_2O_3 (R = Dy, Ho, Er). Since $Cu_2Yb_2O_5$ is also a member of the $Cu_2R_2O_5$ family of compounds whose crystal structure belongs to a noncentrosymmetric space group $P2_1nb$, an attempt has been made to correlate their thermodynamic properties such as enthalpy and entropy of formation with the ionic radius of the trivalent rare-earth cation present in octahedral coordination. Based on this correlation, ΔH, ΔS, and ΔG for the formation of $Cu_2Tb_2O_5$, $Cu_2Tm_2O_5$, and $Cu_2Lu_2O_5$ from the component oxides have been estimated.

INTRODUCTION

Rare-earth (R)–Cu–O ternary systems constitute one of the four triangular faces of the quaternary systems R–Ba–Cu–O, which hosts the superconducting compounds $RBa_2Cu_3O_{7-x}$, $R_2Ba_4Cu_7O_{15-x}$, and $RBa_2Cu_4O_8$. Phase relations and thermodynamic properties of interoxide compounds in R–Cu–O ternary systems and R–Ba–Cu–O quaternary systems must be accurately known in order to synthesize phase pure superconducting compounds. Two types of compounds, CuR_2O_4 and $Cu_2R_2O_5$, are found to exist in the R–Cu–O ternary system depending on the ionic radius of the R^{3+} cation. The orthorhombic $CuLa_2O_4$-type of structure (T) gives rise to p-type superconductors (1). The T′-type of CuR_2O_4 compounds are formed for smaller cations (Pr^{3+}–Gd^{3+}) in which the divalent Cu^{2+} has a square planar coordination. For the cations smaller than Gd^{3+}, the T′-type of phase is no longer stable at ambient pressures and a compound of $Cu_2R_2O_5$-type appears. The transformation of T → T′ → 225 types of rare-earth cuprates occurs mainly because of the breaking of the R–O coordination number (2) as the ionic radius of the R^{3+} cation decreases from La → Lu. The coordination number for the rare-earth cation decreases from ninefold in the T-phase, to eightfold in the T′-phase, and finally to sixfold in the 225-phase in order to optimize the Madelung energy of the R–O framework as the ionic radius of the R^{3+} cation decreases.

All the $Cu_2R_2O_5$ compounds crystallize in the orthorhombic structure with the space group $P2_1nb$ and have blue color. The structure can be visualized as a stack of Cu–O layers positioned parallel to the *ab*-plane and separated by layers of rare-earth atoms. Copper has a distorted square planar arrangement of oxygen atoms around it whereas the rare-earth atom occupies a distorted octahedral site. A detailed crystal structure of $Cu_2R_2O_5$ compounds is well documented by Freund and Muller-Buschbaum (3) and more recently by Garcia-Munoz and Rodriguez-Carvajal (4). Garcia-Munoz and Rodringuez-Carvajal (4) have recently applied the valence bond method to calculate the extent of deviation of $Cu_2R_2O_5$

0022-4596/96 $18.00

compounds from the valence sum rule (VSR). Further, they (4) also calculated the global instability index (GII) for each of the $Cu_2R_2O_5$ compounds. Based on these results of calculation, they concluded that the RO_6 octahedra expands from Lu to Tb in the $Cu_2R_2O_5$ compound exactly corresponding to the increase in ionic radius of R^{3+}. Hence the valence bond sums is not altered. On the other hand, they (4) showed that the valence bond sums for Cu^{2+} is approximately 1.8, lower than the theoretical value of 2. This can be attributed to the Jahn–Teller effect by the Cu^{2+} ($3d^9$) cation. The GII calculation (4) indicates that the stability of $R_2Cu_2O_5$, purely from a structural point of view, increases linearly as the ionic radius of the R^{3+} ion decreases. In other words $Cu_2Lu_2O_5$ is most stable whereas $Cu_2Tb_2O_5$ is least stable.

Tretyakov *et al.* (5) have measured the thermodynamic stability of $Cu_2R_2O_5$ (R = Tb, Dy, Er, Yb) between 1173 and 1340 K by the solid oxide galvanic cell technique. From the temperature dependence of the Gibbs energy of formation of $Cu_2R_2O_5$, Tretyakov *et al.* (5) obtained the enthalpy and entropy of formation of $Cu_2R_2O_5$. The enthalpy and entropy of formation of $Cu_2R_2O_5$ from component oxides (5) when plotted as a function of the ionic radius of the R^{3+} cation in octahedral coordination does not show a smooth variation. Further, recent calorimetric determination of the enthalpy of formation of $Cu_2R_2O_5$ (R = Y, Dy, Ho, Er, Tm, Yb, Lu) from CuO and R_2O_3 by Muromachi and Navrotsky (6) also exhibits a similar variation. The enthalpy and entropy of formation from Tretyakov *et al.* (5) and calorimetric enthalpy of formation from Muromachi and Navrotsky (6) are compared in Fig. 1. It is expected that the enthalpy and entropy of formation of the $Cu_2R_2O_5$ family of compounds from CuO and R_2O_3 should be a smooth function of ionic radius of the R^{3+} cation. In order to resolve the inconsistencies between the variation of crystallographic parameters and thermodynamic properties of the $Cu_2R_2O_5$ compounds, we have conducted careful measurements of the Gibbs energy of formation of $Cu_2Dy_2O_5$ (7), $Cu_2Ho_2O_5$ (8), and $Cu_2Er_2O_5$ (9) from the component oxides. As a part of continuing investigation, we have measured the Gibbs energy of formation of $Cu_2Yb_2O_5$ between 960 and 1320 K employing the solid oxide electrochemical cell

$$(-)\mathrm{Pt}/Cu_2O + Yb_2O_3 + Cu_2Yb_2O_5//(CaO)ZrO_2//O_2\ (P = 0.0212\ \mathrm{MPa})/\mathrm{Pt}(+). \quad [\mathrm{I}]$$

An attempt has been made to correlate the enthalpy and entropy of formation of $Cu_2R_2O_5$ (R = Dy, Ho, Er, Yb) from component oxide with the crystal structure.

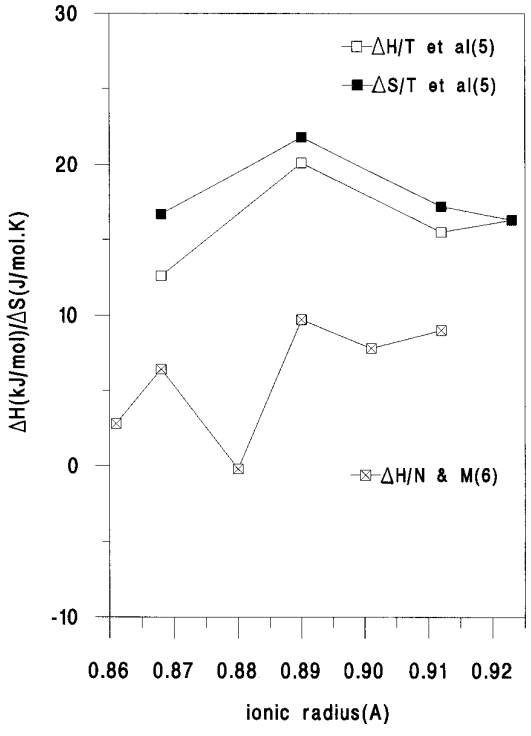

FIG. 1. Enthalpy and entropy change for reaction [11] from literature (5, 6).

EXPERIMENTAL PROCEDURE

Materials

High purity (>99.9%) fine powders of Yb_2O_3 and $CuCO_3 \cdot Cu(OH)_2 \cdot H_2O$ were supplied by Aldrich Chemical Company Ltd. (Gillingham, UK). Cupric oxide was prepared by decomposing the fine powders of basic copper carbonate monohydrate at 800 K for 5 h in air whereas cuprous oxide was synthesized by heating the basic copper carbonate monohydrate in argon atmosphere at 1273 K for 12 h. The blue colored ternary oxide, $Cu_2Yb_2O_5$, was synthesized following the solid-state ceramic route by intimately mixing dried powders of CuO and Yb_2O_3 of submicrometer particle size in 2 : 1 molar ratio and firing the mixture at 1273 K for 48 h in air. The complete formation of $Cu_2Yb_2O_5$ was confirmed by X-ray diffraction analysis using Cu$K\alpha$ radiation. The X-ray diffraction pattern of $Cu_2Yb_2O_5$ did not indicate any peaks due to either unreacted CuO or Yb_2O_3. A high density, impervious grade, fully stabilized $(CaO)ZrO_2$ solid electrolyte tube 450 mm long, 9 mm outer diameter, and 7 mm inner diameter, closed at one end, was supplied by Mandoval Ltd (Lightwater, UK). High purity gases were supplied by BOC (Leeds, UK).

Emf Measurements

A schematic diagram of the cell assembly is shown in Fig. 2. The solid-state cell I is assembled inside a one end

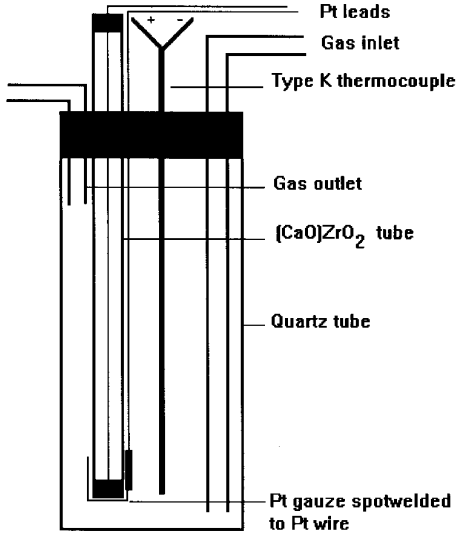

FIG. 2. Schematic diagram of the cell assembly.

closed quartz tube in such a way that the reference and measuring electrode compartments are separated by the solid electrolyte tube. This is found to be essential when the electrodes have significantly high equilibrium oxygen partial pressure. Phase relations in the $Cu–YbO_{1.5}–O$ ternary system suggests that $Cu_2O–Yb_2O_3–Cu_2Yb_2O_5$ is the only three-phase field for which the oxygen potentials as a function of temperature are not known. Therefore the measuring electrode of cell I was prepared by ramming an intimate mixture of $Cu_2O + Yb_2O_3 + Cu_2Yb_2O_5$ inside the solid electrolyte tube with a Pt-lead embedded in the electrode mixture for electrical contact. The measuring electrode of cell I was contained inside the solid electrolyte tube in order to minimize the dead volume over the electrode mixture. The electrode compartment was then evacuated at ambient temperature and sealed under vacuum. This helped rapid attainment of the equilibrium at the electrode. The reference electrode was a flowing dry air free of CO_2 with an oxygen partial pressure of 0.0212 MPa. This was confirmed by a standard cell at 1010 and 1320 K with $CuO + Cu_2O$ as the measuring electrode. The electrical contact to the reference electrode of cell I was made by attaching a Pt-gauze to the outer surface of the closed end of the $(CaO)ZrO_2$ tube with the help of Pt-paint (Engelhardt type A4731). The Pt-gauze was spot-welded to a Pt-lead. The solid-state cell is housed inside a quartz tube and then placed inside the horizontal tube furnace in such a way that the two electrodes are situated in a constant temperature zone in order to avoid any thermo-emf contributions. The outer quartz tube of the cell was wrapped tightly with a fecr-alloy wire of 2 mm diameter which was connected to the ground terminal in order to eliminate the effect of induced emf on the measuring leads. The temperature of the cell was measured by a room temperature compensated K-type thermocouple placed adjacent to the electrodes of the cell. The emf of the cell was measured using a high impedance ($>10^{12}\ \Omega$) Keithley 614 digital electrometer and recorded on an x-t chart recorder. The emf of the cell was measured continuously for 10 days at randomly selected temperatures between 960 and 1320 K. The cell was considered under equilibrium only when the emf of the cell was stable within ± 0.2 mV for at least 10–18 h depending on the temperature of measurement. The stable value of emf was reproducible on thermal cycling and after short-circuiting the cell at selected temperatures of measurement indicating the reversibility of the electrodes.

RESULTS

The measured emf of cell I at different temperatures is given in Table 1 and the variation of the emf of cell I as a function of temperature is shown in Fig. 3. The least-squares regression analysis of the measured emf of cell I gives

$$E_{\mathrm{I}} = 599.03 - 0.427T\,(\pm 0.5)\ \mathrm{mV}. \qquad [1]$$

The numbers and letters along the best-fit line in Fig. 3

TABLE 1
Measured Emf of Cell I as a Function of Temperature

T(K)	E(mV)
1142.0	111.1
1143.0	111.3
1145.0	111.1
1145.0	111.0
1055.0	148.5
962.0	188.5
1190.0	91.1
1187.0	92.2
1189.0	91.3
1192.0	91.1
1277.0	53.1
1280.0	52.8
1280.0	52.6
1280.0	52.6
1277.0	53.1
1101.0	129.0
1006.0	169.5
1311.0	39.7
1311.0	39.9
1236.0	73.2
1233.0	73.3
1144.0	111.1
1141.0	110.9
1145.0	110.9

indicates the sequence of emf measurements in two different runs. According to the Nernst equation, the emf of the solid-state electrochemical cell I is related to the partial pressure of oxygen at the two electrodes by the expression

$$E_I = \frac{RT}{nF}\int_{P''_{O_2}}^{P'_{O_2}} t_{O^{2-}}\, d(\ln P_{O_2}). \qquad [2]$$

In Eq. [2], R is the universal gas constant, T is the temperature in K, n is the number of electrons participating in the electrode reaction, F is the Faraday constant, $t_{O^{2-}}$ is the transport number of O^{2-} ions in $(CaO)ZrO_2$ solid electrolyte, P'_{O_2} and P''_{O_2} are the equilibrium oxygen partial pressures at the reference and measuring electrode, respectively, and E_I is the measured emf of cell I. Since the transport number of oxygen ions in $(CaO)ZrO_2$ is greater than 0.99 (10) for the temperature and oxygen partial pressure range covered in this study, the emf of cell I is directly proportional to the logarithm of the ratio of partial pressure of oxygen at the two electrodes at constant temperature. At the reference electrode of cell I,

$$O_2(g) + 4e^- \rightarrow 2O^{2-} \qquad [3]$$

and at the measuring electrode,

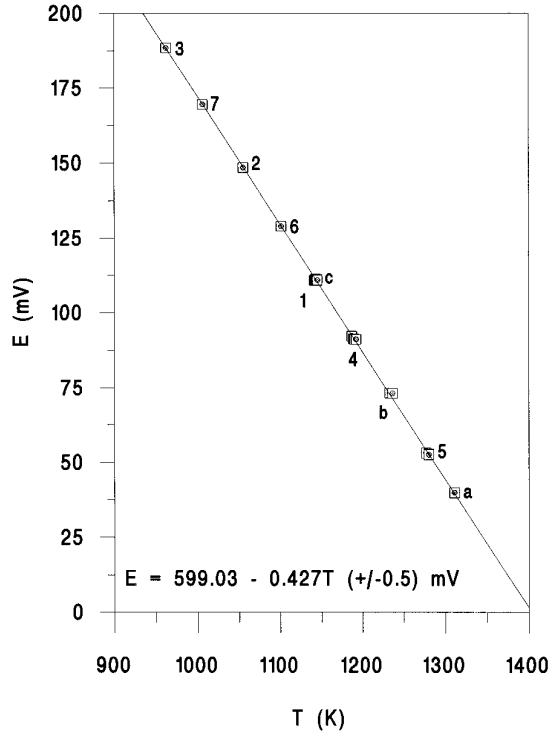

FIG. 3. Temperature dependence of the emf of cell I.

TABLE 2
Comparison of Gibbs Energy Change for Reaction [5] with the Results of Tretyakov *et al.* (5)

	ΔG°_5 (J mol^{-1})	
T(K)	Ref. (5)	Present study
973		−83,478
1073		−68,293
1173	−54,305	−53,108
1273	−38,078	−37,924
1320	−30,452	−30,787

$$2Cu_2O(s) + 2Yb_2O_3(s) + 2O^{2-} \rightarrow 2Cu_2Yb_2O_5(s) + 4e^- \qquad [4]$$

Combining reactions [3] and [4] gives the overall cell reaction

$$2Cu_2O(s) + 2Yb_2O_3(s) + O_2(g) \rightarrow 2Cu_2Yb_2O_5(s). \qquad [5]$$

Substituting the measured emf of cell I and the partial pressure of oxygen at the reference electrode (0.21 atm) in Eq. [2] gives

$$\Delta G^\circ_5 = -231{,}225 + 151.847T\,(\pm 200)\ \text{J mol}^{-1}. \qquad [6]$$

DISCUSSION

Gibbs energy of formation of $Cu_2Yb_2O_5$ from component oxides can be obtained by combining Eq. [6] with the Gibbs energy change for the reaction

$$2Cu_2O(s) + O_2(g) \rightarrow 4CuO(s) \qquad [7]$$

given by the expression

$$\Delta G^\circ_7 = -265{,}482 + 192T\,(\pm 200)\ \text{J mol}^{-1}. \qquad [8]$$

The Gibbs energy change for reaction [7] obtained in this study agrees with the results of Jacob and Alcock (11) and Pankratz (12). Combining Eq. [6] and Eq. [8] gives the Gibbs energy change for the reaction

$$2CuO(s) + Yb_2O_3(s) \rightarrow Cu_2Yb_2O_5(s) \qquad [9]$$

expressed by the equation

$$\Delta G^\circ_9 = 17{,}128 - 20.072T\,(\pm 100)\ \text{J mol}^{-1}. \qquad [10]$$

The results obtained in this investigation are compared with those of Tretyakov *et al.* (5) in Table 2. It can be seen

from Table 2 that the Gibbs energy change for reaction [5] obtained in the present investigation agrees well with the results of Tetyakov *et al.* (5). However, the enthalpy and entropy change for reaction [5] obtained by Tretyakov *et al.* (5) are significantly different from those obtained in the present investigation. It is evident from Eq. [2] that the slope of the linear relationship between emf and temperature of a solid oxide electrochemical cell yields entropy change for the net cell reaction and correspondingly the enthalpy change for the net cell reaction is obtained from the intercept of the linear relationship between emf and temperature. Therefore, more accurate values of enthalpy and entropy change for reaction [5] can be obtained if the emf of cell I is measured over a wider temperature range. Since Tretyakov *et al.* (5) conducted the measurements over a very narrow temperature range, we believe that their results may not be accurate. More conclusive evidence of the accuracy of data can be provided by the "third law" analysis of the Gibbs energy change for reaction [5]. This requires the additional data on heat capacity of all the species involved in reaction [5] at high and low temperatures. Since the heat capacity data for $Cu_2Yb_2O_5$ is not available in the literature, the third law analysis cannot be done.

The Gibbs energy of formation of $Cu_2R_2O_5$ (R = Dy, Ho, Er), reported earlier by Kale and co-workers (7–9), and that of $Cu_2Yb_2O_5$ obtained in this study, from the component oxides, gives the enthalpy and entropy change for the reaction

$$2CuO(s) + R_2O_3(s) \rightarrow Cu_2R_2O_5(s) \qquad [11]$$

for R = Dy, Ho, Er, and Yb. As mentioned earlier, in $Cu_2R_2O_5$-type of compounds the R^{3+} ion is situated in octahedral site. Therefore the enthalpy and entropy change for reaction [11] is plotted as a function of ionic radius of the R^{3+} cation in octahedral coordination in Fig. 4. It can be clearly seen that the enthalpy and entropy change for reaction [11] are both positive and increase linearly as the ionic radius of R^{3+} increases. A positive enthalpy change for reaction [11] probably arises as a result of large distortion of coordination polyhedra around Cu^{2+} in $Cu_2R_2O_5$ compared to that in tenorite (CuO). The distortion of the coordination polyhedra around Cu^{2+} ions increases as the ionic radius of the R^{3+} cation increases in $Cu_2R_2O_5$ compounds (4). This means that the enthalpy of formation of $Cu_2R_2O_5$ from component oxides must become more and more positive as the ionic radius of R^{3+} increases. This is exactly shown in Fig. 4.

The ionic radius of the R^{3+} cation in octahedral coordination varies smoothly in the lanthanide series (13) indicating a smooth contraction from La to Lu. A similar smooth contraction of RO_6 octahedra in $Cu_2R_2O_5$ is also observed (4). Further, the valence bond sums for different $Cu_2R_2O_5$ compounds are also shown to have a constant value of 3 for the rare earth (4). This clearly indicates that there is no evidence of crystal field effect on electrons in the $4f$ orbitals of the octahedrally coordinated R^{3+} cation. However, in case of the first transition metal series, the ionic radius of divalent M^{2+} cations do not conform to smooth variation of lanthanides (13). The characteristic twin peak curve has been explained by crystal field theory (14–17). In $Cu_2R_2O_5$ the valence bond sums for Cu^{2+} gives a value of 1.8 approximately which is lower than the theoretical value of 2 because of the Jahn–Teller effect (4). This clearly suggests that there may be a significant entropy contribution to $Cu_2R_2O_5$ due to the Jahn–Teller effect in $Cu_2R_2O_5$ as in the case of the $MgAl_2O_4$-type of spinels (18).

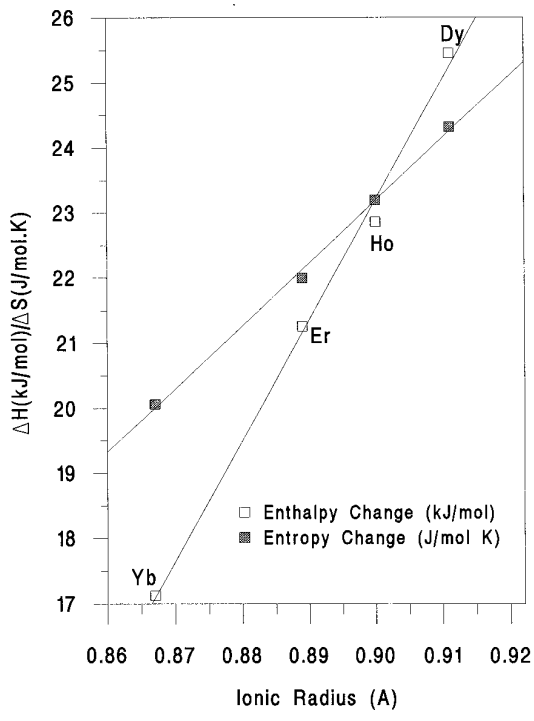

FIG. 4. Variation of the enthalpy and entropy change for reaction [11] as a function of the ionic radius of R^{3+} in octahedral coordination.

There does not exist any report in the literature on either high temperature cation distribution in $Cu_2R_2O_5$ compounds or any data on high temperature X-ray diffraction. Assuming that there is negligible cation mixing at high temperature in $Cu_2R_2O_5$, the configurational entropy contribution is negligible. Further, assuming that the d orbitals of the Cu^{2+} ($3d^9$) ion are oriented randomly at elevated temperature the Jahn–Teller entropy contribution due to the presence of Cu^{2+} ions in $Cu_2R_2O_5$ can be given by the expression (18)

$$\Delta S^{JT} = \text{nR1n 3 J mol}^{-1}\text{ K}^{-1}. \qquad [12]$$

In Eq. [12], ΔS^{JT} is the Jahn–Teller entropy, n is the number of moles of Jahn–Teller cations, and R is the universal gas constant. Since there are two moles of Cu^{2+} ions per mole of $Cu_2R_2O_5$, the value of ΔS^{JT} is equal to 18.27 J mol^{-1} K^{-1}. The value of ΔS^{JT} is always positive hence it may be concluded that the stability of the $Cu_2R_2O_5$ structure is enhanced due to the Jahn–Teller effect. This clearly explains the high entropy change for the solid state reaction [11] obtained experimentally for different rare earths. In the absence of the Jahn–Teller effect, the entropy change for the solid state reaction [11] will be reasonably small as expected.

The results shown in Fig. 4 permits us to estimate the Gibbs energy of formation of $Cu_2Tb_2O_5$, $Cu_2Tm_2O_5$, and $Cu_2Lu_2O_5$. The temperature dependence of the estimated Gibbs energy of formation of $Cu_2R_2O_5$ (R = Tb, Tm, Lu) according to reaction [11] is given by the expressions

$$\Delta G_f^\circ\langle Cu_2Tb_2O_5\rangle = 27{,}290 - 25.32T\,(\pm 100)\ \text{J mol}^{-1}, \quad (13)$$

$$\Delta G_f^\circ\langle Cu_2Tm_2O_5\rangle = 19{,}315 - 21.17T\,(\pm 100)\ \text{J mol}^{-1}, \quad (14)$$

and

$$\Delta G_f^\circ\langle Cu_2Lu_2O_5\rangle = 15{,}792 - 19.33T\,(\pm 100)\ \text{J mol}^{-1}. \quad (15)$$

The thermodynamic stability of $Cu_2R_2O_5$ relative to its component oxides decreases as the ionic radius of the R^{3+} cation increases for R = Tb to Lu. This agrees with the results obtained by Garcia-Munoz and Rodriguez-Carvajal (4) purely from the structural parameters.

CONCLUSIONS

The Gibbs energy of formation of $Cu_2Yb_2O_5$ has been measured by the solid oxide electrochemical technique between 960 and 1320 K. The present results combined with the earlier measurements of Kale and co-workers (7–9) gives an excellent correlation between ΔH and ΔS for reaction [11] and the ionic radius of R^{3+} in octahedral site of $Cu_2R_2O_5$ (R = Dy, Ho, Er, Yb). The high entropy of formation of $Cu_2R_2O_5$ from component oxides is explained in terms of the Jahn–Teller effect in $Cu_2R_2O_5$ compounds. The data on ΔH and ΔS presented in Fig. 4 is used to estimate the Gibbs energy of formation of $Cu_2Tb_2O_5$, $Cu_2Tm_2O_5$, and $Cu_2Lu_2O_5$ from component oxides.

ACKNOWLEDGMENTS

The author thanks EU for financial support and Miss N. Townson for her assistance in preparing the manuscript.

REFERENCES

1. J. G. Bednorz and K. A. Muller, *Z. Phys. B* **64,** 189 (1986).
2. J. F. Bringley, S. Trail, and B. Scott, *J. Solid State Chem.* **86,** 310 (1990).
3. H. R. Freund and H. Muller-Buschbaum, *Z. Naturforsch. B* **32,** 609 (1977).
4. J. L. Garcia-Munoz and J. Rodriguez-Carvajal, *J. Solid State Chem.* **115,** 324 (1995).
5. Yu. D. Tretyakov, A. R. Kaul, and N. V. Makukhin, *J. Solid State Chem.* **17,** 183 (1976).
6. E. Takayama-Muromachi and A. Navrotsky, *J. Solid State Chem.* **106,** 349 (1993).
7. G. M. Kale, *J. Am. Ceram. Soc.* (1995), communicated.
8. G. M. Kale and D. J. Fray, *J. Mater. Res.* (1995), communicated.
9. G. M. Kale and D. J. Fray, *Mater. Res. Bull.* (1995), communicated.
10. J. W. Patterson, *J. Electrochem. Soc.* **118,** 1033 (1971).
11. K. T. Jacob and C. B. Alcock, *J. Am. Ceram. Soc.* **8,** 192 (1975).
12. L. B. Pankratz, "Thermodynamic Properties of Elements and Oxides," Bulletin 672, p. 131, 133. U.S. Bureau of Mines, 1982.
13. R. G. Burns, "Mineralogical Applications of Crystal Field Theory" (A. Putnis and R. C. Liebermann, Eds.), 2nd ed., p. 241, 242. Cambridge Univ. Press, Cambridge, 1993.
14. J. H. van Santen and J. S. van Wieringen, *Rec. Trav. Chem. Pay.-Bas.* **71,** 420 (1952).
15. N. S. Hush and M. H. L. Pryce, *J. Chem. Phys.* **26,** 143 (1957).
16. N. S. Hush and M. H. L. Pryce, *J. Chem. Phys.* **28,** 424 (1958).
17. N. S. Hush, *Disc. Faraday Soc.* **26,** 145 (1958).
18. K. S. Irani, A. B. P. Sinha, and A. B. Biswas, *Proc. Phys. Soc. London* **71,** 270 (1958).